Enhancement of Visual Perception with Use of Dynamic Cues[1]

Marcelo E. Andia, MD, MSc
Johannes Plett, MSc[2]
Cristian Tejos, PhD
Marcelo W. Guarini, PhD
María E. Navarro, MD
Dravna Razmilic, MD
Luis Meneses, MD
Manuel J. Villalon, PhD
Pablo Irarrazaval, PhD

Institutional review board approval and signed informed consent were not needed, as medical images included in public databases were used in this study. The purpose of this study was to improve the detection of microcalcifications on mammograms and lung nodules on chest radiographs by using the dynamic cues algorithm and the motion and flickering sensitivity of the human visual system (HVS). Different sets of mammograms from the Mammographic Image Analysis Society database and chest radiographs from the Japanese Society of Radiological Technology database were presented statically, as is standard, and in a video sequence generated with the dynamic cues algorithm. Nine observers were asked to rate the presence of abnormalities with a five-point scale (1, definitely not present; 5, definitely present). The data were analyzed with receiver operating characteristic (ROC) techniques and the Dorfman-Berbaum-Metz method. The video sequence generated with the dynamic cues algorithm increased the rate of detection of microcalcifications by 10.2% ($P = .002$) compared with that obtained with the standard static method, as measured by the area under the ROC curve. Similar results were obtained for lung nodules, with an increase of 12.3% ($P = .0054$). The increase in the rate of correct detection did not come just from the image contrast change produced by the algorithm but also from the fact that image frames generated with the dynamic cues algorithm were put together in a video sequence so that the motion sensitivity of the HVS could be used to facilitate the detection of low-contrast objects.

Supplemental material: *http://radiology.rsnajnls.org/cgi/content/full/250/2/551/DC1*

[1] From the Department of Radiology (M.E.A., M.E.N., D.R., L.M.), Biomedical Imaging Center (M.E.A., C.T., M.W.G., L.M., P.I.), Department of Electrical Engineering (J.P., C.T., M.W.G., P.I.), and Faculty of Biological Sciences (M.J.V.), Pontificia Universidad Católica de Chile, Marcoleta 367, 2° Piso, Santiago 8330024, Chile. Received January 25, 2008; revision requested April 26; revision received August 1; final version accepted September 23. Supported by FONDECYT (grant no. 1070674) and FONDEF (grant no. D05I10358). **Address correspondence to** M.E.A. (e-mail: *mandia@med.puc.cl*).

[2] **Current address:** Department of Systems and Computational Neurobiology, Max-Planck-Institute of Neurobiology, Martinsried, Germany.

The human vision system (HVS) is a powerful tool used to improve image perception and processing. Nevertheless, there are some cases in which it is difficult for the HVS to detect an object if the background is of similar intensity or texture, as is often the case with medical images. Classic examples of this are mammograms with microcalcifications and chest radiographs with lung nodules. Mammograms tend to have low contrast, and microcalcifications tend to be small; these factors make it difficult to detect microcalcifications on mammograms (1) and result in a false-negative rate of up to 20% in screening tests (2). It is difficult to detect lung nodules because of poor image contrast between lesions and healthy tissue and because of the potential overlap of lesions with the ribs, heart, or other chest structures (2), resulting in a false-negative rate of up to 50% in screening tests (3).

One approach that may help in the detection of lesions is the use of a computer-aided detection system (4–9), in which the software automatically presents possible abnormalities to the observer. Another approach is to visually enhance lesions without making any decision about the potential presence of abnormalities. For example, contralateral subtraction (10) is used to subtract a mirrored version of the same image and enhances any asymmetry as a highly visible hyperintense region. Another example is color digital summation (11), which is used to transform gray-scale images into color-coded images. This method highlights potential abnormalities, making them highly visible because of the color sensitivity of the HVS.

To our knowledge, we are the first to use HVS sensitivity to motion and flickering in image interpretation, despite the fact that this sensitivity is a useful diagnostic tool. Our work is based on what the HVS is capable of detecting and the concept that the HVS is sensitive to amplitude, motion, and flicker (12). Amplitude sensitivity is used to view static scenes, where differences of intensity or color can be interpreted as objects, textures, et cetera. This kind of sensitivity has been widely studied (13) and implicitly used in almost all aspects of traditional image analysis, including analysis of traditional medical images.

Motion sensitivity deals with the detection of moving objects, and it is easily explained by evolution. It has always been crucial to survival for animals, including humans, to be able to detect moving predators and prey. Indeed, most cortical cells of the HVS respond better to moving objects than to stationary ones (14). Similarly, flicker sensitivity is used to detect temporally modulated stimuli.

The purpose of this study was to improve the detection of microcalcifications on mammograms and lung nodules on chest radiographs by using the dynamic cues algorithm and the motion and flickering sensitivity of the HVS.

Advances in Knowledge

- It is possible to use dynamic cues to transform static images into video sequences so that motion or flickering sensitivity of the human vision system is used to analyze medical images.
- Use of dynamic cues results in a substantial increase in the correct detection of microcalcifications on mammograms and lung nodules on chest radiographs.

Implications for Patient Care

- The improvement in the detection of microcalcifications and lung nodules achieved with the dynamic cues algorithm could positively affect the sensitivity of screening programs for breast and lung cancer.
- The dynamic cues algorithm enabled more accurate diagnosis than did standard static observation and involved use of the same imaging technology, without extra costs to the patients.

Materials and Methods

Institutional review board approval and signed informed consent were not needed, as the entire study was performed with medical images included in public databases. When we wished to use motion or flickering sensitivity to assess the images, we introduced spatial or temporal motion to the images, thereby converting them to video sequences. To introduce spatial motion, we moved portions of the image (typically only the pixels) in space. To introduce temporal motion, the pixel did not move in space; however, its intensity changed over time. There are several ways to introduce artificial movement to images. The method presented herein is based on three consecutive processes: a motion process, an observation process, and a computation process, in which dynamic cues are computed (Fig 1). The observation process sets the parameters for the type of motion that will be implemented, the motion process specifies the type of movement that will be applied to the original image, and the computation process sets the dynamic cues that will be presented to the observer.

Observation Process

The purpose of the observation stage is to process the original image to establish the parameters that will govern the motion process. In other words, it is a process in which one can define which features of the original

Published online
10.1148/radiol.2502080168

Radiology 2009; 250:551–557

Abbreviations:
AUC = area under the ROC curve
HVS = human vision system
ROC = receiver operating characteristic

Author contributions:
Guarantors of integrity of entire study, M.E.A., M.W.G., P.I.; study concepts/study design or data acquisition or data analysis/interpretation, all authors; manuscript drafting or manuscript revision for important intellectual content, all authors; manuscript final version approval, all authors; literature research, M.E.A., J.P., C.T., M.E.N., D.R., L.M., M.J.V., P.I.; clinical studies, J.P., L.M., P.I.; statistical analysis, M.E.A., J.P., M.W.G., M.J.V., P.I.; and manuscript editing, all authors

Authors stated no financial relationship to disclose.

image will show more or less motion or flicker in the final dynamic cues video sequence.

There are different observation processes that can be applied. The simplest process is to observe the original intensity of each pixel. High-signal-intensity pixels will have larger variations in motion or flicker than will low-signal-intensity pixels. Other observation processes are the use of high-pass frequency filters, which will produce larger variations in small features or edges; wavelet transformations, which will produce larger variations in certain sizes and frequencies on the original image; or any kind of linear or nonlinear filtering that results in an image or a region of interest that has the same dimensions as the original image.

Motion Process

The purpose of the motion process is to create a sequence of image frames (all of which are the same size) in which the intensity of each pixel varies over time and follows a pattern of movement that is computed with the parameters obtained during the observation process. This movement can be temporal (referred to as flicker) or spatial.

Figure 2 shows a possible use for spatial movement as a sideways oscillation of every pixel at a constant amplitude and frequency depending on the inverse of the original intensity of each pixel. In this way, a dark pixel may oscillate from one side to the other faster than a lighter pixel. Another way to introduce spatial motion is with pulsating motion, as shown in Figure 3. The frequency of pulsations depends on the inverse of the original intensity of each pixel. These two implementations require some kind of interpolation in image space, as well as a rule for dealing with occlusion. The maximum amount

Figure 1

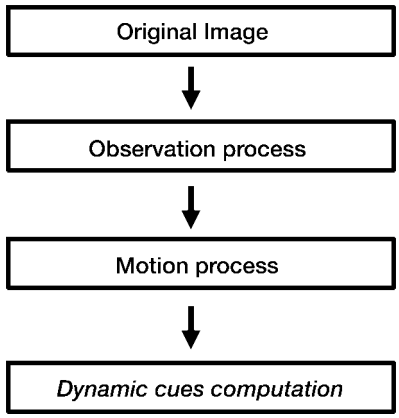

Figure 1: Flowchart shows the dynamic cues computation process.

Figures 2–4

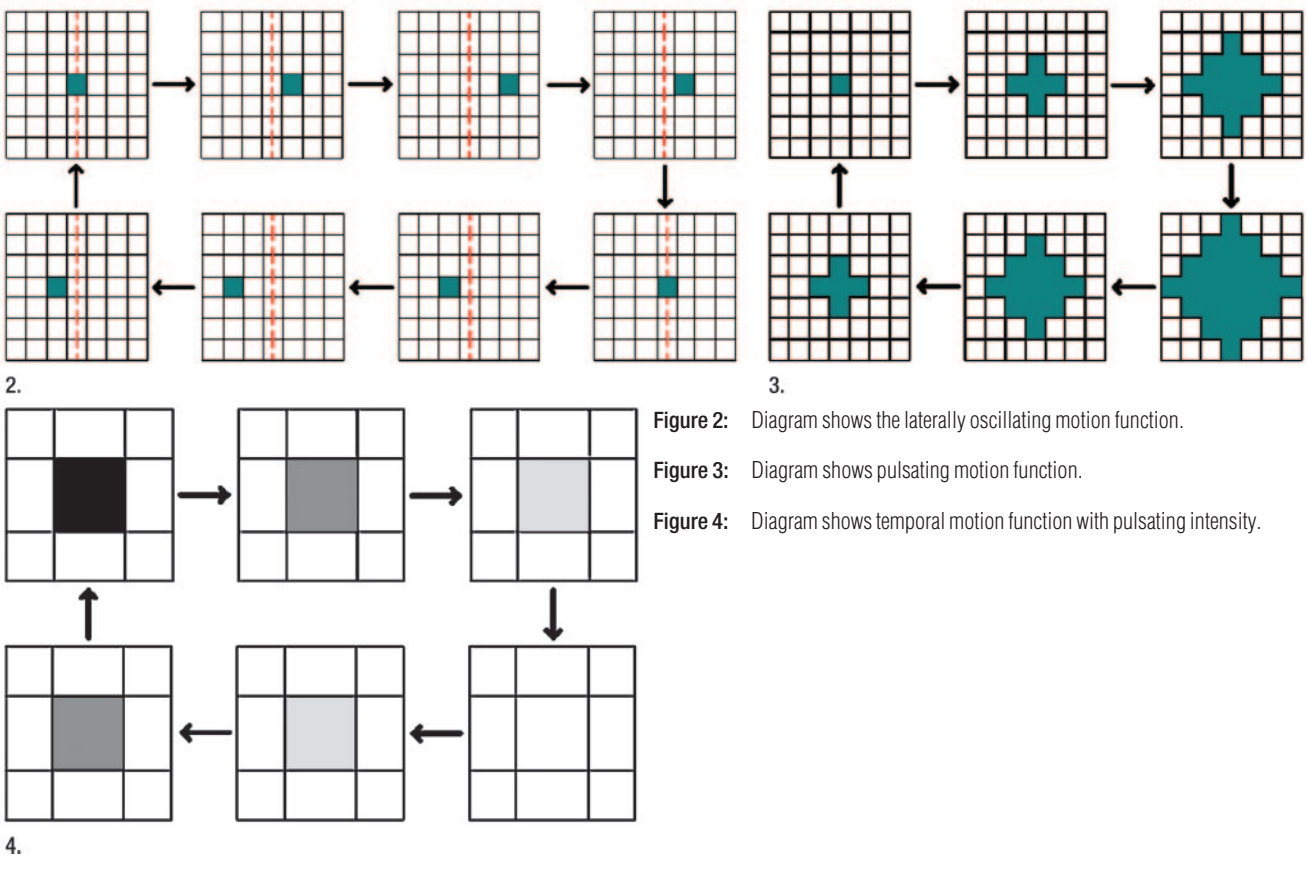

Figure 2: Diagram shows the laterally oscillating motion function.

Figure 3: Diagram shows pulsating motion function.

Figure 4: Diagram shows temporal motion function with pulsating intensity.

of movement described by the pixels can be adjusted as a tuning parameter of the chosen type of spatial movement.

Temporal movement can be achieved by varying the intensity of each pixel, whereas the frequency of variation again depends on the computations performed for every pixel during the observation process. A simple example is shown in Figure 4, where the intensity of a pixel varies as sinusoidal function with a frequency that depends on its original intensity. Different temporal or spatial motion patterns can be created by using different periodic functions, such as sine, triangular, and rectangular waves.

Computation Process

In the computation process, the intensity of pixels in each frame of the final dynamic cues sequence video is computed as a weighted average between the original image and the frame given by the motion process. In this way, irrelevant features reveal only small changes when compared with the original images, and the majority of the motion or flickering stimuli are produced by important features of the image. The whole process of generating the dynamic cues video sequence with a standard personal computer takes less than 1 minute.

When viewing the whole array of images as a movie, it is possible to detect objects by using the phase shift produced between two pixels with different original intensities. Even if these two adjacent pixels have relatively small differences in intensity on the original image, in time the phase shift (in this case introduced by temporal motion) will become visible, as shown in Figure 5, where two pixels with a minimal intensity difference produce a phase shift of 180° at some point. In some aspects, this is similar to dynamically changing image contrast, which is a frequently used tool in medical imaging. Here, the viewer is presented with a sequence of images in which the contrast changes nonlinearly.

Figure 6, *A*, shows a mammogram with a cluster of microcalcifications that have small differences in gray-scale intensity with respect to normal tissue (as can be seen in Figure 6, *B*, and in the gray-scale intensity profile of Figure 6, *C*). To perceive the effect on the HVS, this should be seen as a movie; however, some of the effects produced by the dynamic cues algorithm can be appreciated by plotting the intensity pixels corresponding to microcalcifications and their neighborhood as a function of time. In Figure 7, each line represents a specific time frame for the relation intensity versus the pixel location. Clearly, the pixels that experience the largest intensity variations over time are those that correspond to microcalcifications, and it is this particular variation that excites the HVS.

One may think that choosing the right time frame (where the difference in intensity between microcalcifications and neighboring healthy tissue is highest) from the nonlinear dynamic cues

Figure 5

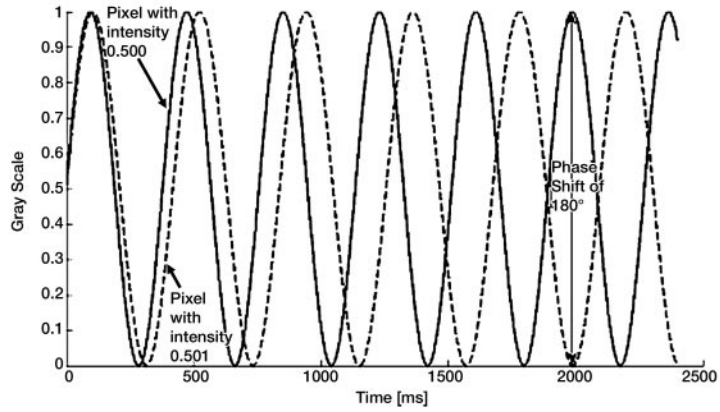

Figure 5: Graph shows phase shift of two pixels with slightly different gray-scale intensities.

Figure 6

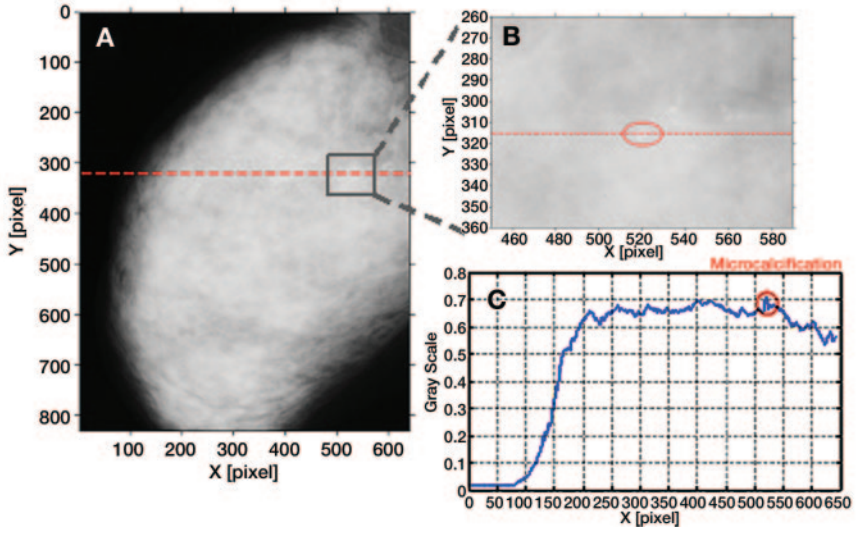

Figure 6: *A*, Mammogram with microcalcifications. *B*, Magnified view of the microcalcification. *C*, Gray-scale intensity profile of the dashed line in *A* shows the gray-scale contrast between the microcalcification and the normal tissue.

algorithm could be enough to enable an observer to detect the abnormality; however, as we will demonstrate, it is the flickering effect of a blinking region in a video sequence that produces the major benefits in terms of visual detection. A mathematic modeling of these three processes is given in Appendix E1 *(http://radiology.rsnajnls.org/cgi/content/full/250/2/551/DC1)*.

Validation of the Dynamic Cues Hypothesis

To compare diagnostic results of analysis performed with and without the dynamic cues algorithm, we designed a test in which the observer evaluated a set of static images (standard static test), a set of images with all of the frames generated with the dynamic cues algorithm in a static fashion (static adjustment test), and a set of images generated with the dynamic cues algorithm in a dynamic fashion (dynamic cues test). We used mammograms taken from the Mammographic Image Analysis Society database *(http://wiau.man.ac.uk/services/MIAS/MIASweb.html)* (15) and chest radiographs taken from the digital image database of the Japanese Society of Radiological Technology *(http://jsrt.or.jp/english.html)* (16).

In the standard static test, a set of 100 images was chosen from the previously mentioned databases. This set included 50 mammograms (20 with microcalcifications, 30 with normal findings that served as controls) and 50 chest radiographs (20 with lung nodules, 30 with normal findings that served as controls).

In the static adjustment test, a set of 30 static frames was prepared for each of the 100 images, with use of the flickering option of the dynamic cues algorithm. The observers could review each set of static frames in whichever order they chose, with a 10-second gap between individual frames during which a black screen appeared so that observers could not see two images consecutively. In this way, the dynamic cue effect was avoided.

In the dynamic cues test, a video sequence was put together for each image by using the same 30 static frames from the previous test so that images from the second and third tests were identical except that images in the latter test were presented dynamically. In all three tests, the data sets were randomly rearranged, and observers analyzed them on different days (between 2 and 30 days of separation).

Five experienced radiologists (D.R., M.E.N.; 24 and 18 years of experience, respectively) performed mammographic tests, whereas four 3rd-year radiology residents performed chest radiographic tests. Observers rated the presence of microcalcifications or lung nodules with a five-point scale: (1, definitely not present; 5, definitely present). Radiologists and residents were trained in image interpretation with a 3-minute video clip that showed them three video sequences generated with the dynamic cues algorithm. One sequence was of a normal image, and the remaining two were of images with microcalcifications or lung nodules. Finally, all radiologists and residents were asked to give an overall impression of the dynamic cues algorithm in terms of its utility and how comfortable they felt during the test.

Data Analysis

Receiver operating characteristic (ROC) analysis was used to compare observer performance in the detection of lung nodules and microcalcifications in the three tests. The areas under the ROC curve (AUCs) were computed with a quasi–maximum likelihood estimation of the binormal distribution by using the computer program DBM MRMC 2.2 *(http://krl.bsd.uchicago.edu/KRE_ROC/software_index.htm)*, which was provided by Metz and colleagues (17,18). The significance of the difference in AUC between the dynamic cues experiments and each of the two static experiments was estimated with the Dorfman-Berbaum-Metz method (18). This method included assessment of reader variation and case sample variation with analysis of variance (19,20).

Figure 7

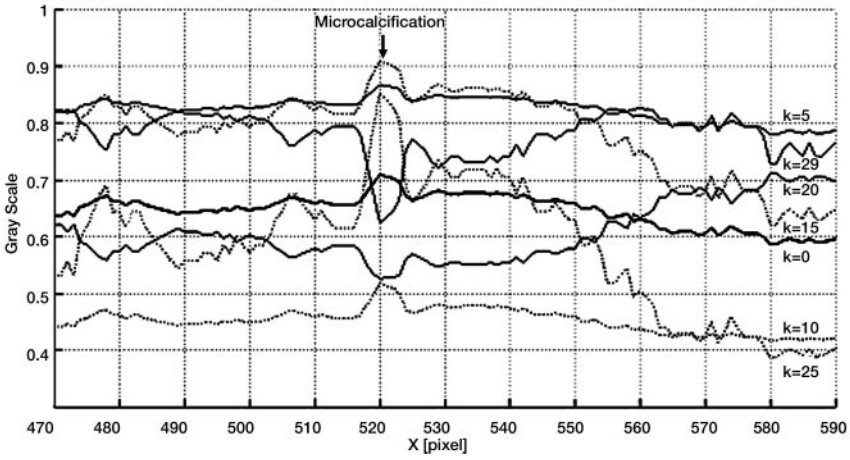

Figure 7: Graph shows gray-scale intensity distribution of the dashed line in Figure 6, *A*, in a specific time frame versus pixel location.

Results

Since it is impossible to show the visual effects of dynamic cues just by using static images on paper, example videos with dynamic cues for mammograms and chest radiographs are available on our Web site *(www.mri.cl/dynamiccues)*. We have also included two example videos with this article (Movies 1, 2, *http://radiology.rsnajnls.org/cgi/content/full/250/2/551/DC1*).

Tables 1 and 2 show the AUCs used to analyze accuracy in the detection of microcalcifications on mammograms and lung nodules on chest radiographs for all three implemented tests. The dynamic cues test increased

the AUC for all observers when compared with that obtained with the standard static method or the static adjustment method. In the detection of microcalcifications, the dynamic cues method increased the AUC by 10.2% (P = .002) compared with the standard static method and by 5.3% (P = .043) compared with the static adjustment method. In the detection of lung nodules, on average, the dynamic cues method increased the AUC by 12.3% (P = .0054) compared with the standard static method and by 10.4% (P = .018) compared with the static adjustment method.

In terms of the qualitative analysis performed by radiologists and residents, all observers agreed that the dynamic cues algorithm was useful, as the video sequence generated with the dynamic cues algorithm enabled them to confirm some diagnostic doubts and distinguish some lesions that were not identified on the static images. Three of the nine observers, however, indicated that they felt tired by the end of the test because the images strained their eyes.

Discussion

The main strength of the dynamic cues method lies in its ability to exploit highly evolved brain functions that are already present in humans but have not been used previously to analyze medical images (21), without discarding traditional static two-dimensional brain functions. The dynamic cues algorithm exposes observers to different visual stimuli (intensity, motion, and flickering) and enables them to better distinguish low-contrast objects.

It may be difficult for an observer to detect abnormalities on medical images because of the camouflage effect. Humans can be easily tricked by objects with the right camouflage (ie, if they have textures or colors similar to those of the background). In these cases, we can actually see the object of interest because of our visual intensity sensitivity, but we cannot distinguish it from the rest of the field of view. Well-camouflaged and still objects become distinguishable only when they start to move differently than the background because our visual system is adapted to recognize spatial or temporal movement (13).

Similarly, it is difficult for readers to spot microcalcifications on mammograms or lung nodules on chest radiographs because these abnormalities have intensities and textures similar to those in the image background. Thus, the dynamic cues algorithm consists of a nonlinear process that introduces specific kinds of motion to static images so that we can show the observer movies in which structures move with different patterns, and abnormalities become easily distinguishable.

There is strong evidence in the literature that shows that the HVS is partic-

Table 1

AUC Values in the Detection of Microcalcifications on Mammograms

Observer and Overall Average	Standard Static Test (%)*	Static Adjustment Test (%)*	Dynamic Cues Test (%)*	Difference between Dynamic Cues Test and Standard Static Test (%)	Difference between Dynamic Cues Test and Static Adjustment Test (%)
Radiologist 1	89.2	94.2	98.1	8.9	3.9
Radiologist 2	88.7	92.0	97.9	9.2	5.9
Radiologist 3	78.1	89.0	94.9	16.8	5.9
Radiologist 4	85.5	87.7	95.4	9.9	7.7
Radiologist 5	89.1	91.9	95.1	6.0	3.2
Average	86.1	91.0	96.3	10.2	5.3

Note.—P values were calculated with the Dorfman-Berbaum-Metz method and were as follows: .002 for the difference between dynamic cues test and standard static test and .043 for the difference between dynamic cues test and static adjustment test.

* Data are AUCs.

Table 2

AUC Values in the Detection of Lung Nodules on Chest Radiographs

Observer and Overall Average	Standard Static Test (%)*	Static Adjustment Test (%)*	Dynamic Cues Test (%)*	Difference between Dynamic Cues Test and Standard Static Test (%)	Difference between Dynamic Cues Test and Static Adjustment Test (%)
Resident 1	81.3	89.7	92.5	11.2	2.8
Resident 2	72.7	72.9	82.6	9.9	9.7
Resident 3	72.0	70.0	88.4	16.4	18.4
Resident 4	74.6	75.6	86.3	11.7	10.7
Average	75.1	77.0	87.4	12.3	10.4

Note.—P values were calculated with the Dorfman-Berbaum-Metz method and were as follows: .0054 for the difference between dynamic cues test and standard static test and .018 for the difference between dynamic cues test and static adjustment test.

* Data are AUCs.

ularly sensitive to visual motion stimuli. Several functional magnetic resonance imaging experiments have shown that visual motion stimuli activate additional cerebral areas beyond those activated by static visual stimuli (22–25). These additional activation areas are the ones that might be responsible for the improvement in the detection of microcalcifications and lung nodules with use of dynamic cues.

Perhaps the main weakness inherent in the use of dynamic cues is the strain on the eyes caused by exposure to flicker for prolonged periods. About one-third of observers said that viewing mammograms or radiographs with dynamic cues for more than 30 minutes without a break was tiring. This was mainly attributed to the pulsating intensity motion function used to generate the sequences. The choice of other periodic wave functions in the motion process generally tends to put less strain on the eyes but results in less contrast. To overcome this weakness, better wave functions have to be investigated. Another weakness is the inexperience and lack of training of radiologists in this way of evaluating images; however, this should not be a substantial limitation once the dynamic cues technique becomes a widely available and used method.

It is important to note that the improvement in the detection of microcalcifications and lung nodules achieved with use of the dynamic cues algorithm could positively affect the sensitivity of screening programs for breast and lung cancer, as this technique can be used to assign a diagnosis that is more accurate than that assigned with the standard static observation and makes use of the same imaging technology without extra costs for the patients.

References

1. Sickles EA. Breast calcifications: mammographic evaluation. Radiology 1986;160(2):289–293.
2. Tan BB, Flaherty KR, Kazerooni EA, Iannettoni MD. The solitary pulmonary nodule. Chest 2003;123(1 suppl):89S–96S.
3. Elmore JG, Armstrong K, Lehman CD, Fletcher SW. Screening for breast cancer. JAMA 2005;293(10):1245–1256.
4. Ge J, Sahiner B, Hadjiiski LM, et al. Computer aided detection of clusters of microcalcifications on full field digital mammograms. Med Phys 2006;33(8):2975–2988.
5. H Jamarani S, Rezai-Rad G, Behnam H. A novel method for breast cancer prognosis using wavelet packet based neural network. Conf Proc IEEE Eng Med Biol Soc 2005;4:3414–3417.
6. Regentova E, Zhang L, Zheng J, Veni G. Microcalcification detection based on wavelet domain hidden markov tree model: study for inclusion to computer aided diagnostic prompting system. Med Phys 2007;34(6):2206–2219.
7. Campadelli P, Casiraghi E, Artioli D. A fully automated method for lung nodule detection from postero-anterior chest radiographs. IEEE Trans Med Imaging 2006;25(12):1588–1603.
8. Shiraishi J, Abe H, Li F, Engelmann R, MacMahon H, Doi K. Computer-aided diagnosis for the detection and classification of lung cancers on chest radiographs ROC analysis of radiologists' performance. Acad Radiol 2006;13(8):995–1003.
9. Schilham AM, van Ginneken B, Loog M. A computer-aided diagnosis system for detection of lung nodules in chest radiographs with an evaluation on a public database. Med Image Anal 2006;10(2):247–258.
10. Tsukuda S, Heshiki A, Katsragawa S, Li Q, MacMahon H, Doi K. Detection of lung nodules on digital chest radiographs: potential usefulness of a new contralateral subtraction technique. Radiology 2002;223(1):199–203.
11. Ogata Y, Naito H, Tomiyama N, et al. Evaluation of usefulness of color digital summation radiography for solitary pulmonary nodules on chest radiographs. Radiat Med 2006;24(5):351–357.
12. Lu Z, Lin W, Yang X, Ong E, Yao S. Modeling visual attention's modulatory aftereffects on visual sensitivity and quality evaluation. IEEE Trans Image Process 2005;14(11):1928–1942.
13. Wandell BA. Foundations of vision. Sunderland, Mass: Sinauer Associates, 1995.
14. Hubel D. Eye, brain, and vision. Oxford, England: Scientific American Library, 1988.
15. Suckling J, Parker J, Dance D, et al. The Mammographic Image Analysis Society digital mammogram database. Excerpta Medica International Congress Series 1994;1069:375–378.
16. Shiraishi J, Katsuragawa S, Ikezoe J, et al. Development of a digital image database for chest radiographs with and without a lung nodule: receiver operating characteristic analysis of radiologists' detection of pulmonary nodules. AJR Am J Roentgenol 2000;174(1):71–74.
17. Metz CE. Some practical issues of experimental design and data analysis in radiological ROC studies. Invest Radiol 1989;24(3):234–245.
18. Dorfman DD, Berbaum KS, Metz CE. Receiver operating characteristic rating analysis: generalization to the population of readers and patients with the jackknife method. Invest Radiol 1992;27(9):723–731.
19. Hillis SL, Berbaum KS. Power estimation for the Dorfman-Berbaum-Metz method. Acad Radiol 2004;11(11):1260–1273.
20. Dorfman DD, Berbaum KS, Lenth RV, Chen YF, Donaghy BA. Monte Carlo validation of a multireader method for receiver operating characteristic discrete rating data: factorial experimental design. Acad Radiol 1998;5(9):591–602.
21. Huber DE, Healey CG. Visualizing data with motion. Proceedings of IEEE Visualization Conference. Los Alamitos, Calif: Institute of Electrical and Electronics Engineers, 2005; 67.
22. Bartram L, Ware C, Calvert T. Moticons: detection, distraction and task. Int J Hum Comput Stud 2003;58(5):515–545.
23. Carmel D, Lavie N, Rees G. Conscious awareness of flicker in humans involves frontal and parietal cortex. Curr Biol 2006;16(9):907–911.
24. Moutoussis K, Zeki S. Seeing invisible motion: a human FMRI study. Curr Biol 2006;16(6):574–579.
25. Sunaert S, Van Hecke P, Marchal G, Orban GA. Motion-responsive regions of the human brain. Exp Brain Res 1999;127(4):355–370.

Radiology 2009

This is your reprint order form or pro forma invoice

(Please keep a copy of this document for your records.)

Reprint order forms and purchase orders or prepayments must be received 72 hours after receipt of form either by mail or by fax at 410-820-9765. It is the policy of Cadmus Reprints to issue one invoice per order. **Please print clearly**.

Author Name _____
Title of Article _____
Issue of Journal_____ Reprint # _____ Publication Date _____
Number of Pages_____ KB # _____ Symbol Radiology
Color in Article? Yes / No (Please Circle)

Please include the journal name and reprint number or manuscript number on your purchase order or other correspondence.

Order and Shipping Information

Reprint Costs **(Please see page 2 of 2 for reprint costs/fees.)**

_____ Number of reprints ordered $_____
_____ Number of color reprints ordered $_____
_____ Number of covers ordered $_____
Subtotal $_____
Taxes $_____

(*Add appropriate sales tax for Virginia, Maryland, Pennsylvania, and the District of Columbia or Canadian GST to the reprints if your order is to be shipped to these locations*.)

First address included, add $32 for each additional shipping address $_____

TOTAL $_____

Shipping Address **(cannot ship to a P.O. Box) Please Print Clearly**

Name _____
Institution _____
Street _____
City _____ State _____ Zip _____
Country _____
Quantity_____ Fax _____
Phone: Day _____ Evening _____
E-mail Address _____

Additional Shipping Address* **(cannot ship to a P.O. Box)**

Name _____
Institution _____
Street _____
City _____ State _____ Zip _____
Country _____
Quantity _____ Fax _____
Phone: Day _____ Evening _____
E-mail Address _____

** Add $32 for each additional shipping address*

Payment and Credit Card Details

Enclosed: Personal Check _____
Credit Card Payment Details _____

Checks must be paid in U.S. dollars and drawn on a U.S. Bank.

Credit Card: __ VISA __ Am. Exp. __ MasterCard
Card Number _____
Expiration Date_____
Signature: _____

Please send your order form and prepayment made payable to:

Cadmus Reprints
P.O. Box 751903
Charlotte, NC 28275-1903

Note: Do not send express packages to this location, PO Box.

FEIN #:541274108

Invoice or Credit Card Information

Invoice Address **Please Print Clearly**

Please complete Invoice address as it appears on credit card statement

Name _____
Institution _____
Department _____
Street _____
City _____ State _____ Zip _____
Country _____
Phone _____ Fax _____
E-mail Address _____

Cadmus will process credit cards and *Cadmus Journal Services* will appear on the credit card statement.

If you don't mail your order form, you may fax it to 410-820-9765 with your credit card information.

Signature _____ Date _____

Signature is required. By signing this form, the author agrees to accept the responsibility for the payment of reprints and/or all charges described in this document.

RB-1/01/09

Radiology 2009

Black and White Reprint Prices

Domestic (USA only)						
# of Pages	50	100	200	300	400	500
1-4	$239	$260	$285	$303	$323	$340
5-8	$379	$420	$455	$491	$534	$572
9-12	$507	$560	$651	$684	$748	$814
13-16	$627	$698	$784	$868	$954	$1,038
17-20	$755	$845	$947	$1,064	$1,166	$1,272
21-24	$878	$985	$1,115	$1,250	$1,377	$1,518
25-28	$1,003	$1,136	$1,294	$1,446	$1,607	$1,757
29-32	$1,128	$1,281	$1,459	$1,632	$1,819	$2,002
Covers	$149	$164	$219	$275	$335	$393

International (includes Canada and Mexico)						
# of Pages	50	100	200	300	400	500
1-4	$299	$314	$367	$429	$484	$546
5-8	$470	$502	$616	$722	$838	$949
9-12	$637	$687	$852	$1,031	$1,190	$1,369
13-16	$794	$861	$1,088	$1,313	$1,540	$1,765
17-20	$963	$1,051	$1,324	$1,619	$1,892	$2,168
21-24	$1,114	$1,222	$1,560	$1,906	$2,244	$2,588
25-28	$1,287	$1,412	$1,801	$2,198	$2,607	$2,998
29-32	$1,441	$1,586	$2,045	$2,499	$2,959	$3,418
Covers	$211	$224	$324	$444	$558	$672

Color Reprint Prices

Domestic (USA only)						
# of Pages	50	100	200	300	400	500
1-4	$247	$267	$385	$515	$650	$780
5-8	$297	$435	$655	$923	$1194	$1467
9-12	$445	$563	$926	$1,339	$1,748	$2,162
13-16	$587	$710	$1,201	$1,748	$2,297	$2,843
17-20	$738	$858	$1,474	$2,167	$2,846	$3,532
21-24	$888	$1,005	$1,750	$2,575	$3,400	$4,230
25-28	$1,035	$1,164	$2,034	$2,986	$3,957	$4,912
29-32	$1,186	$1,311	$2,302	$3,402	$4,509	$5,612
Covers	$149	$164	$219	$275	$335	$393

International (includes Canada and Mexico))						
# of Pages	50	100	200	300	400	500
1-4	$306	$321	$467	$642	$811	$986
5-8	$387	$517	$816	$1,154	$1,498	$1,844
9-12	$574	$689	$1,157	$1,686	$2,190	$2,717
13-16	$754	$874	$1,506	$2,193	$2,883	$3,570
17-20	$710	$1,063	$1,852	$2,722	$3,572	$4,428
21-24	$1,124	$1,242	$2,195	$3,231	$4,267	$5,300
25-28	$1,320	$1,440	$2,541	$3,738	$4,957	$6,153
29-32	$1,498	$1,616	$2,888	$4,269	$5,649	$7028
Covers	$211	$224	$324	$444	$558	$672

Minimum order is 50 copies. For orders larger than 500 copies, please consult Cadmus Reprints at 800-407-9190.

Reprint Cover

Cover prices are listed above. The cover will include the publication title, article title, and author name in black.

Shipping

Shipping costs are included in the reprint prices. Domestic orders are shipped via FedEx Ground service. Foreign orders are shipped via a proof of delivery air service.

Multiple Shipments

Orders can be shipped to more than one location. Please be aware that it will cost $32 for each additional location.

Delivery

Your order will be shipped within 2 weeks of the journal print date. Allow extra time for delivery.

Tax Due

Residents of Virginia, Maryland, Pennsylvania, and the District of Columbia are required to add the appropriate sales tax to each reprint order. For orders shipped to Canada, please add 7% Canadian GST unless exemption is claimed.

Ordering

Reprint order forms and purchase order or prepayment is required to process your order. Please reference journal name and reprint number or manuscript number on any correspondence. You may use the reverse side of this form as a proforma invoice. Please return your order form and prepayment to:

Cadmus Reprints
P.O. Box 751903
Charlotte, NC 28275-1903

Note: Do not send express packages to this location, PO Box.
FEIN #:541274108

Please direct all inquiries to:

Rose A. Baynard
800-407-9190 (toll free number)
410-819-3966 (direct number)
410-820-9765 (FAX number)
baynardr@cadmus.com (e-mail)

Reprint Order Forms and purchase order or prepayments must be received 72 hours after receipt of form.